

# DFT + U Study of structural, electronic, optical and magnetic properties of LiFePO<sub>4</sub> Cathode materials for Lithium-Ion batteries

A.K. Wabeto, K.N. Nigussa\*, L.D. Deja

*Department of Physics, Addis Ababa University, P.O. Box 1176, Addis Ababa, Ethiopia*

---

## Abstract

In this study, we have employed a DFT+U calculation using quantum-espresso (QE) code to investigate the structural, electronic, optical, and magnetic properties of LiFePO<sub>4</sub> cathode material for Li-ion batteries. Crystals of LiFePO<sub>4</sub> and related materials have recently received a lot of attention due to their very promising use as cathodes in rechargeable lithium-ion batteries. The structural optimization was performed and the equilibrium parameters such as the lattice constants, and the bulk modulus are calculated using QE code and found to be  $a=4.76 \text{ \AA}$ ,  $b=6.00 \text{ \AA}$ ,  $c=10.28 \text{ \AA}$ ,  $\beta = 90.2 \text{ GPa}$ , respectively. The projected density of states (PDOS) for the LiFePO<sub>4</sub> material is remarkably similar to experimental results in literature showing the transition metal  $3d$  states forming narrow bands above the O  $2p$  band. The results of the various spin configurations suggested that the ferromagnetic configuration can serve as a useful approximation for studying the general features of these systems. In the absence of Li, the majority spin transition metal  $3d$  states are well-hybridized with the O  $2p$  band in FePO<sub>4</sub>. The result obtained with a DFT + U showed that LiFePO<sub>4</sub> is direct band gap materials with a band gap of 3.82 eV, which is within the range of the experimental values. The PDOS analyses show qualitative information about the crystal field splitting and bond hybridization and help rationalize the understanding of the structural, electronic, optical, and magnetic properties of the LiFePO<sub>4</sub> as a novel cathode material. On the basis of the predicted optical absorbance, reflection, refractive index, and energy loss function, LiFePO<sub>4</sub> is demonstrated to be viable and cost-effective, which is very suitable as a cathode material for Li-ion battery.

*Keywords:* Lithium-Iron phosphate, Battery, Density functional theory, Cathode.

---

## 1. Introduction

Energy storage is a critical problem in the 21<sup>st</sup> century. As the world population grows, so too does the demand for energy and energy storage materials. The development of the next generation of cars, personal electronics, and renewable energy sources hinges on improvements in battery technology. Batteries are one of the most promising energy storage technologies due to their high conversion efficiency and essentially zero emissions [1]. Lithium-ion batteries (LIBs) are considered to be one of the most promising batteries owing to their high power density, long cycle life, and environmental friendliness, which leads to their wide use in portable electronic devices [2]. The cathode material is the most crucial component of LIBs. Therefore, tremendous efforts have been dedicated to the development of cathode materials. The cathode materials of LIBs are usually intercalation compounds, including layered LiMO<sub>2</sub>, (M=Co, Ni, Mn), LiNi<sub>1-x</sub>Co<sub>x</sub>Mn<sub>y</sub>, spinel LiMn<sub>2</sub>O<sub>4</sub> and olivine LiFePO<sub>4</sub> materials. Among them, olivine-structured LFP was proposed in 1997 by Pandhi [3] with excellent cycling stability, low cost, and good safety. Nevertheless, the poor ionic and electronic conductivity and low Li<sup>+</sup> diffusion has hindered its further application. Morphology control, particle size reduction, surface coatings, and cation or anion doping have been applied to improve its properties [4]. Furthermore, it is significant to explicitly understand the microscopic origins of these improvements.

---

\*Corresponding author: kenate.nemera@aau.edu.et (K.N. Nigussa)

Email address: lemi.demeyu@aau.edu.et (L.D. Deja)

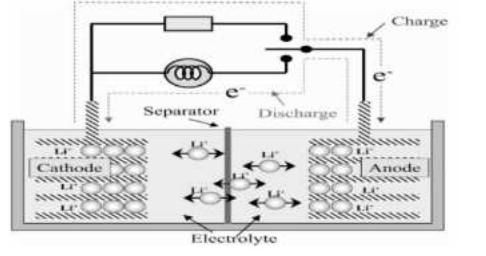
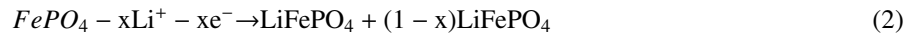
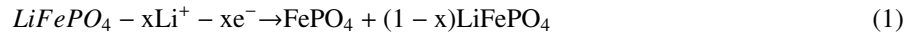


Figure 1: Schematic representation of a common Li-ion battery.

Lithium iron phosphate, which is an ordered type compound, is under extensive studies as one of the most promising cathode material. It has more favored properties such as low cost, environmental compatibility, less toxicity, high thermal stability, and high specific capacity compared to the  $\text{LiCo}_2$  and  $\text{LiMn}_2\text{O}_4$ . Most exciting advantages of  $\text{LiFePO}_4$  is its stability with high voltage application, hardly changes while Li-ion intercalation and deintercalation. In Li-ion battery, lithium ions are extracted from anode to cathode during discharge process and it is reversed during charging as depicted in Fig 1. The extraction and insertion of lithium during charging and recharging process may be written as Eqs. (1) & (2) below. However, the poor intrinsic electronic and ionic conductivities of  $\text{LiFePO}_4$  limits its practical use. Moreover, the band-gap of  $\text{LiFePO}_4$  is under debate which requires more structural and electronic analysis [5, 6].



Even though the low cost, good stability, and competitive electrochemical properties make the olivine  $\text{Li}_x\text{MPO}_4$  family an exciting new area for cathode development in Li rechargeable batteries, they are facing challenges due to their low electrical conductivity. Among these olivine cathode materials,  $\text{LiFePO}_4$ , which is in its pure form has very poor conductivity, greatly inhibited high-rate applications. Efforts to increase conductivity of electrodes made from the materials have focused on particle size reduction, intimate carbon coating, and cation doping. Significant disagreement exists on the origin of the low electronic conductivity [7].

Ab-initio studies focusing on the band gap and effective hole or electron mass have found a small gap, or no gap at the Fermi level, which seems to be in contradiction to experiment. However, there is significant evidence that the local density approximation (LDA) and generalized gradient approximation (GGA) used in almost all previous studies on the electronic structure of these phosphates cannot accurately reproduce their electronic structure due to the approximate treatment of the electron correlation in transition metal orbitals by LDA/GGA. In order to clarify the electronic structure of  $\text{LiFePO}_4$  we have applied the more accurate DFT+U (LDA+U/GGA+U) method to determine the projected density of states (PDOS) of these materials [8].

Concerns with the safety, cost, charge/discharge rates, cycle life, and energy density of Li-ion batteries represent the main challenges in Li-ion development. Additionally, if Li-ion batteries are to be employed in Hybrid Electrical Vehicles (HEVs) then gravimetric energy density, uniformity in performance of individual cells inside a complex, multicell battery, and cost are the fields where more research is absolutely necessary [9]. Thus, current rapid development of society requires a major advancement in the battery materials to achieve high accuracy, long life cycle, low cost, and reliable safety. Therefore, many new efficient energy storage materials and battery systems are being developed and explored, and their working mechanisms must be clearly understood before industrial applications [10]. Nowadays, computers are very useful tools for condensed matter physics and material sciences and they have been used to predict the electronic, optical, and magnetic properties of materials by using a suitable computing method [11]. By now, a lot of first principle calculations have been performed on  $\text{LiFePO}_4$  cathode materials and  $\text{FePO}_4$  [12] to analyze electronic, optical, and magnetic properties of  $\text{LiFePO}_4$ . The focus of this study was the electronic structure

calculation and analysis of optical, and magnetic properties for LiFePO<sub>4</sub> and end material of LiFePO<sub>4</sub>, FePO<sub>4</sub> within density functional theory (DFT) frame work. From many aspects, iron is an attractive metal for use in the field of battery materials since it is abundant and environmentally friendly [13]. Crystals of LiFePO<sub>4</sub> and related materials have recently received a lot of attention due to their very promising use as cathodes in rechargeable lithium ion batteries [14].

The paper is organized as follows. In the next section (sec. 2), a detail account of the computational method is presented. Results and discussion are presented in section 3, with the conclusion being presented in section 4.

## 2. Computational Methods

An ab-initio simulations within quantum espresso code [15] is used to examine the electronic structure and optical properties of LiFePO<sub>4</sub>. The electron wave-function is expanded over a plane wave basis set. The electron-ion interactions is approximated within projector augmented wave (PAW) modality [16] upon the calculation of electronic properties and geometry optimization. Upon optical properties calculations, the electron-ion interactions is approximated within norm conserving pseudopotential [17]. The exchange-correlation energies are treated using PBE [18]. The k-points of the Brillouin zone (BZ) are generated from the input **k**-mesh using the Monkhorst-Pack scheme [19].

The number of valence electrons considered for each element within the paw data sets is Li:1, Fe:8, P:5, and O:6. Geometry relaxations are carried out using BFGS minimizer [20], where optimization of the atomic coordinates and the unit cell degrees of freedom is done within the concept of the Hellmann-Feynman forces and stresses [21, 22] as calculated on the Born-Oppenheimer (BO) surface [23]. The convergence criteria for the forces were set at 0.05 eV/Å. A van der Waal's treatment within DFT-D3 [24] is applied wherever necessary. The **k**-mesh of 4×4×4 and a cut-off energy (ecut) of 600 eV is used in the calculations.

Hubbard U correction [25] is applied to the dopant atoms. We have selected U=4.5 eV to be optimum to our system. Spin polarized calculation is allowed. Density of states (DOS) is calculated as a population of states in the spin-up and spin-down states at the chosen energy windows. Projected DOS (PDOS) is calculated as a component of DOS resolved onto atomic orbitals. To characterize optical properties, a dielectric function is computed, which has generally a complex nature & is given as

$$\varepsilon(\omega) = \varepsilon_1(\omega) + i \varepsilon_2(\omega) \quad (3)$$

The imaginary part  $\varepsilon_2(\omega)$  is calculated from the density matrix of the electronic structure [26] as described elsewhere [27], & given by

$$\varepsilon_2(\omega) = \frac{8\pi^2 e^2 \hbar^2}{\Omega \omega^2 m_e^2} \sum_{k,v,c} w_k |\langle \psi_k^c | \mathbf{u} \cdot \mathbf{r} | \psi_k^v \rangle|^2 \delta(E_k^c - E_k^v - \hbar\omega), \quad (4)$$

where  $e$  is the electronic charge, and  $\psi_k^c$  and  $\psi_k^v$  are the conduction band (CB) and valence band (VB) wave functions at  $\mathbf{k}$ , respectively,  $\hbar\omega$  is the energy of the incident phonon,  $\mathbf{u} \cdot \mathbf{r}$  is the momentum operator,  $w_k$  is a joint density of states, &  $\Omega$  is volume of the primitive cell. The real part  $\varepsilon_1(\omega)$  can be extracted from the imaginary part  $\varepsilon_2(\omega)$  (Eq. (4)) according to Kramer-Kronig relationship [28], as follows.

$$\varepsilon_1(\omega) = 1 + \frac{2}{\pi} P \int_0^{\infty} \frac{\omega' \varepsilon_2(\omega')}{\omega'^2 - \omega^2} d\omega' \quad (5)$$

where  $P$  is a principal value. The electron energy loss function ( $L(\omega)$ ), as given elsewhere [29], is calculated by

$$L(\omega) = \frac{\varepsilon_2(\omega)}{\varepsilon_1^2(\omega) + \varepsilon_2^2(\omega)} \quad (6)$$

The index of refraction is given by

$$n(\omega) = \frac{1}{\sqrt{2}} \left[ \sqrt{\varepsilon_1^2 + \varepsilon_2^2} + \varepsilon_1 \right]^{1/2} \quad (7)$$

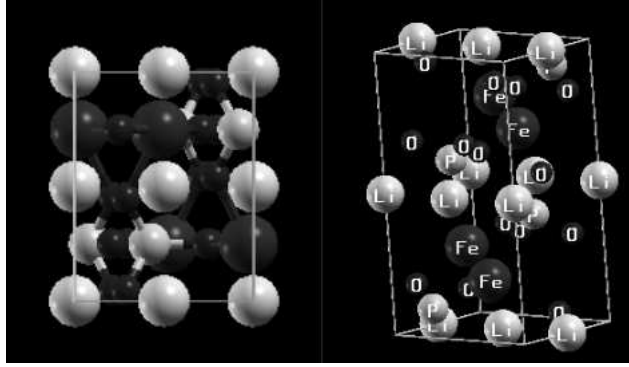


Figure 2: Schematic representations of conventional unit cell for crystalline structure  $\text{LiFePO}_4$  in the olivine structure (a) 2D, and (b) 3D view.

The absorption coefficient is calculated from dielectric function (Eq. (3)) according to

$$\alpha(\omega) = \sqrt{2} \frac{\omega}{c} \left[ \sqrt{\epsilon_1^2 + \epsilon_2^2} - \epsilon_1 \right]^{1/2} \quad (8)$$

An Olivine structured within  $P_{nma}$ , as shown in Fig. 2, is considered in this study where the unit cells contain 28 atoms. On setting up of this structure, literature resources [30–32] have been closely followed. After getting the kinetic energy cut-off and the number of special k-points which give the best convergence possible of total energy, we calculated the total energy for various values of the lattice constants. Energies were calculated for various values of lattice constant, and a curve fitting to the values of total energy as a function of the unit cell volume is done according to Murnaghan equation [33]. From the output of the curve fit, the values of bulk modulus, and lattice constant are predicted.

### 3. Results and Discussion

#### 3.1. Structural and electronic properties

From our DFT calculations, we found the values of the lattice parameters for  $\text{LiFePO}_4$  orthorhombic structure to be  $a = 4.67 \text{ \AA}$ . This result is in good agreement with experimental results in the literature, summarized in Table 1 below.

Table 1: The equilibrium lattice parameters [ $\text{\AA}$ ] of  $\text{LiFePO}_4$  computed from DFT (PBE) and with the DFT + U (PBE + U correction), and compared with available experimental value.

Lattice constant	This work		Experiment [34]	Error (%)
	DFT	DFT + U		
$a$ [ $\text{\AA}$ ]	4.76	4.67	4.71	0.21
$b$ [ $\text{\AA}$ ]	6.00	5.99	5.94	0.84
$c$ [ $\text{\AA}$ ]	10.28	10.36	10.35	0.10

As apparent from Table 1, compared to available experimental data [34], GGA underestimates the equilibrium lattice constant values, while DFT + U produces an optimized unit cell parameters which is in a better agreement with

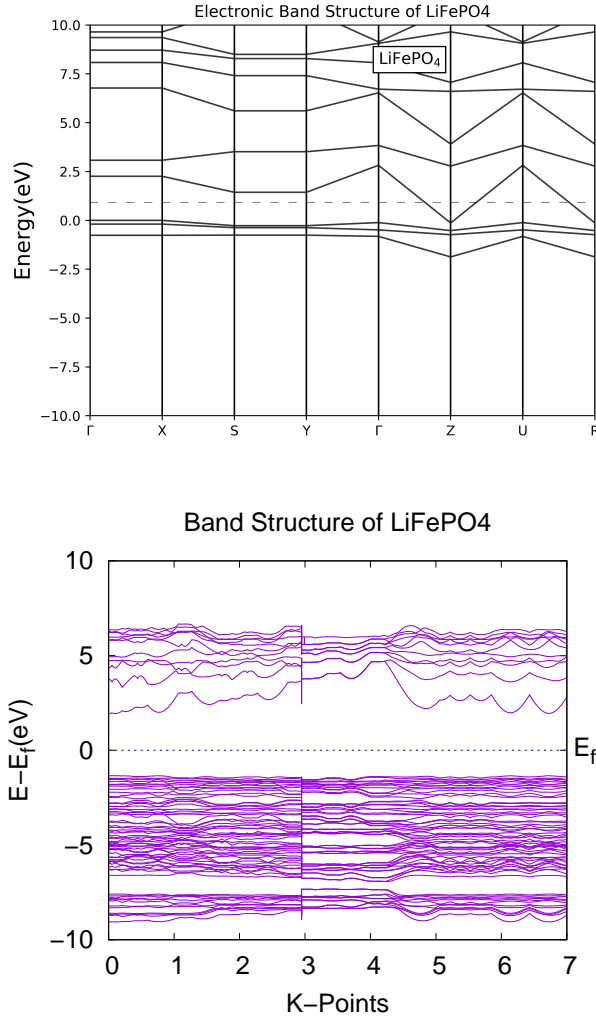


Figure 3: Representations of electronic band structure of LiFePO<sub>4</sub> using (a) DFT and (b) DFT + U functionals.

the experiment data.

The band structure for ferromagnetic forms of FePO<sub>4</sub> and LiFePO<sub>4</sub> are shown in Fig. 3. A direct band gap seems 0.10 eV with DFT (GGA), and 3.82 eV using DFT + U formalism for LiFePO<sub>4</sub>. Experimental band gap results for LiFePO<sub>4</sub> are 2.86-4.00 eV, as reported in a literature [35]. Thus, while the GGA (PBE) functional predicts a metallic behavior with the Fermi level of the system crossing the minority-spin *d* states, DFT + U is effective in predicting a correct band gap. In the total and projected DOS analysis illustrated in Figs. 4 & 5, the main contribution to valence band was associated with O 2*p* states with minor contributions from Fe-3*d* states. At the conduction band, the dominant contribution is by Fe-3*d* atomic orbitals with a small content oxygen atomic orbitals. Thus, it is possible to assume that an electron transfer inside the band gap region should occur between 2*p* orbitals of oxygen atom and 3*d* orbitals of the Fe in tetrahedral configurations, represented by FePO<sub>6</sub> clusters.

In order to know the distribution of the total charge density of LiFePO<sub>4</sub> orthorhombic structure, we have calculated the charge density distribution. From the result we can observe that LiFePO<sub>4</sub> structure makes a covalent bonding. From Fig. 6, it is clear that in LiFePO<sub>4</sub> structure Fe-Fe shows a very weak charge density but when we move to P-P bonding, there is stronger charge density. Also as clear as it is from the scale, purple color shows the greater charge density than the remaining atoms.

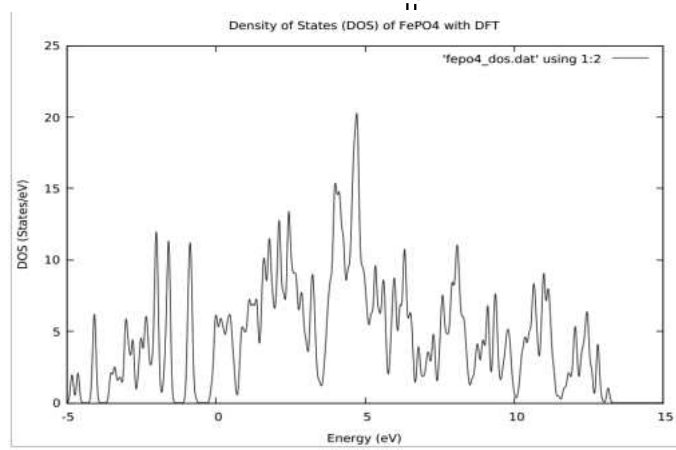
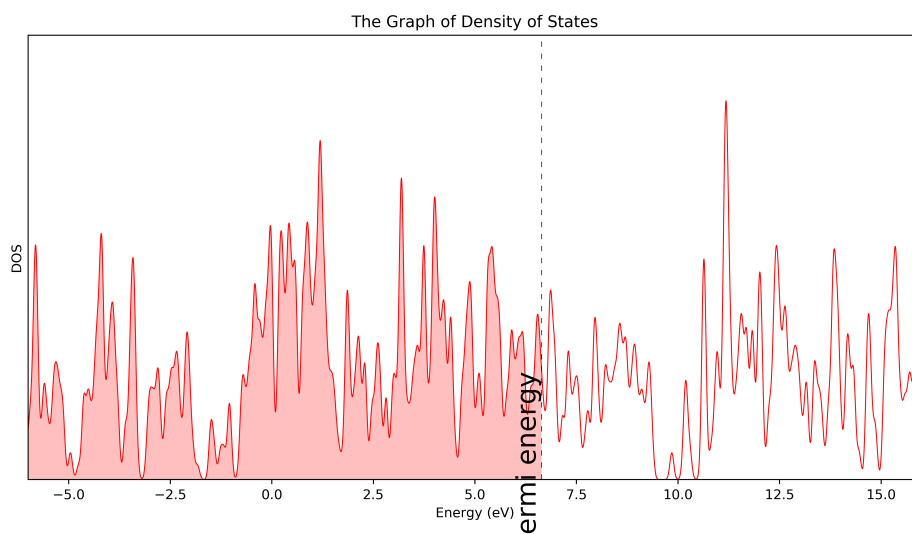


Figure 4: Density of states: (a) FePO<sub>4</sub> and (b) LiFePO<sub>4</sub>.

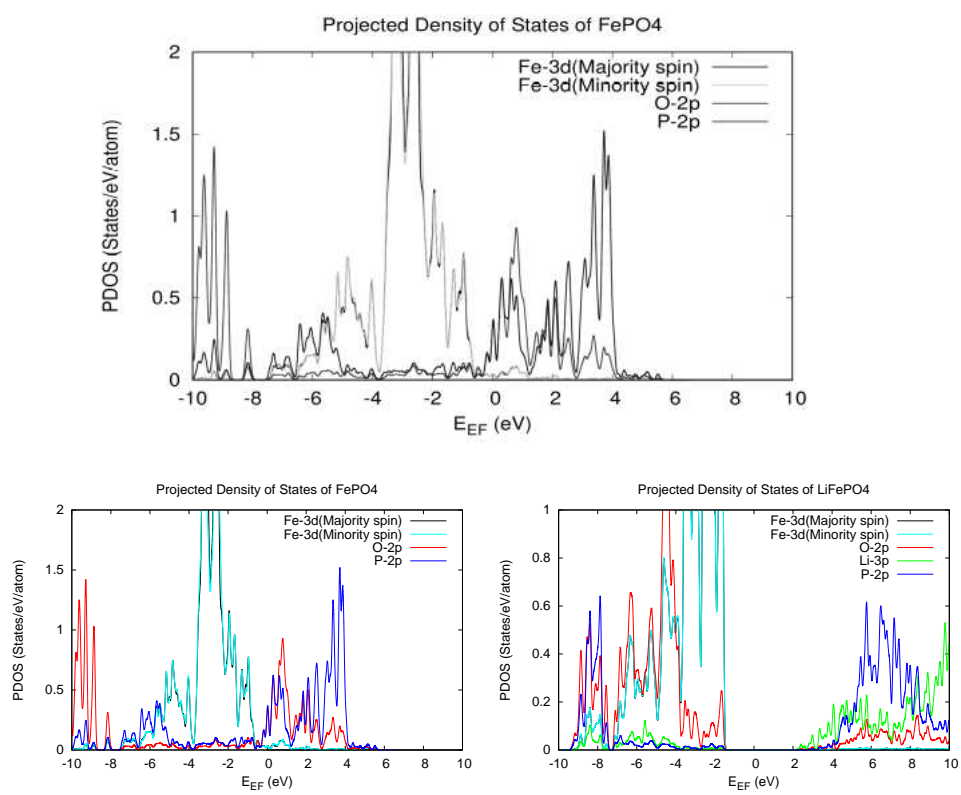


Figure 5: Projected Density of states: (a) FePO<sub>4</sub> and (b) LiFePO<sub>4</sub> using DFT (c) LiFePO<sub>4</sub> using DFT using DFT + U.

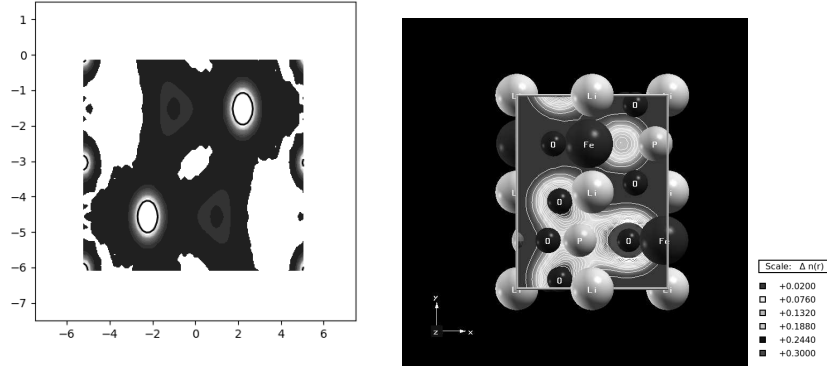


Figure 6: Charge density plot (a) The total charge density plot, and (b) The electronic charge density contour plots for majority electrons in LiFePO<sub>4</sub> in [001] direction, (c) The Thermo scale.

Using Bader decomposition [36], which uses stationary points in the bulk electron density to partition electrons among different atoms, and within the approaches adopted in a literature [37], we have calculated the Bader charges on each atom which are contained within a unit cell of LiFePO<sub>4</sub>, as given in Table 2. The deviation from the ideal

Table 2: Bader Charges values on each atom in LiFePO<sub>4</sub>, where Z means atomic number.

Results of Bader Charge analysis						
Atom	Z	This work	Calc.	Ref. [38]	Error (%)	Nominal charge
Li	3.0	2.12	+0.90	+1.00	10	+1
Fe	16.0	14.5	+1.50	+1.55	3.2	+2
P	5.0	0.12	+4.88	+5.00	2.4	+5
O	6.0	7.83	-1.83	-1.83	0.0	-2
O	6.0	7.87	-1.87	-1.89	1.1	-2
O	6.0	7.90	-1.90	-1.92	1.0	-2

ionic charge density is more significant for Li than for Fe, suggesting a higher degree of covalent in Li – O than in the Fe – O interaction. The homogeneous distribution of contour lines represents the strongly covalent character in the interaction of the Li and Fe cations atoms with oxygen anion on the [001] analyzed plane. The observed behavior occurs because of the hybridization between the O 2*p* atomic orbitals with Fe 3*d* atomic orbitals. For FePO<sub>4</sub>, the Fe states are well hybridized with O 2*p* states throughout the valence band. This is shown both in the projected densities of states plot of Fig. 5 and in the contour plot of Fig. 6.

### 3.2. Optical properties

The optical property of matter can be described by the knowledge of the complex dielectric function, which describes the optical response of the material to the external electromagnetic field [39]. The imaginary part ( $\epsilon_2(\omega)$ )



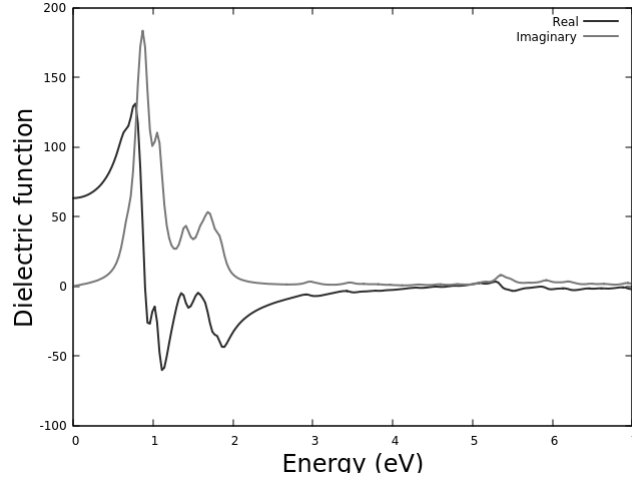


Figure 7: Dielectric function of LFP.

of the dielectric function implies the optical transition mechanism. Each peak in the imaginary part of the dielectric function corresponds to an electronic transition. The imaginary part of the complex dielectric function is related to a measure of optical absorption. The real part of dielectric function is obtained using Eq. (5) and describes other properties such as optical transmission.

Figure 7 depicts a graph of dielectric function against the photon energy which gives the calculated results of the real ( $\epsilon_1$ ) and imaginary ( $\epsilon_2$ ) parts of the dielectric functions which are connected by the dispersion relations [40]. The static value of  $\epsilon_1(0)$  is 64.07, and it reaches a maximum value of 130.27 at photon energy of 0.8 eV. With increasing photon energy, it gradually decreases to a minimum value of -58.98 at photon energy of around 1.12 eV, before it starts to slightly increase again. The distinctive features (peaks) of  $\epsilon_2$  are due to optical transitions involving hybrid O-2p and Fe 3d orbital, as is the case in LiFePO<sub>4</sub> (LFP) [41]. Interestingly in LFP, the band transitions seem to happen without excitonic effects.

The absorption coefficient determines which light of a particular wavelength is absorbed by a material [42]. In a material with a low absorption coefficient, light is only poorly absorbed, and if the material is thin enough, it will appear transparent to that wavelength. The absorption coefficient depends on the material and also on the wavelength of light which is being absorbed. The absorption coefficient of LiFePO<sub>4</sub> is given in Fig. 8. At 2.5 eV, an absorption peak in the *xx*-direction is noticed. At 5.8 eV, an absorption peak in the *zz*-direction is noticed. At 12.5 eV, an absorption peak in the *yy*-direction is noticed.

The refractive index computed using Eq. (7) is shown in Fig. 8. The maximum refractive index value of 14.1 occurs at photon energy of 0.5 eV. The index of refraction at zero photon energy is  $n(0) = 7.9$ . Between photon energies of 0 and 2.0 eV, the index of refraction attains maximum and then gradually decreases to  $n(\omega) = 1$ . Reflectance is ability of a substance to reflect radiation. As shown in Fig. 8, the reflectivity at zero photon energy has values of 0.61 in the *xx*-direction, 0.59 in the *yy*-direction, and 0.72 in the *zz*-direction. At photon energy of 1.84 eV, the highest reflectivity peak of 0.75 is noticed in the *xx*-direction. At photon energy of 1.70 eV, a highest reflectivity peaks of 0.78 in the *zz*-direction and 0.68 in the *yy*-direction is noticed.

The electron energy loss spectrum (eels) displays a prospect of a material resulting in some of the electrons undergoing inelastic scattering, which means that they lose energy and have their paths slightly and randomly deflected. The eels for the LFP system is shown in Fig. 9. At 13.5 eV, we have the highest energy loss in the *xx*-direction.

The Joint density of states (JDOS) is an indicator of the number of available states for photons to interact with. For optical absorption process, it is an important part of optical characteristics of a given material. The JDOS of LFP shows the sharpest peak at 6.0 eV (Fig. 10).

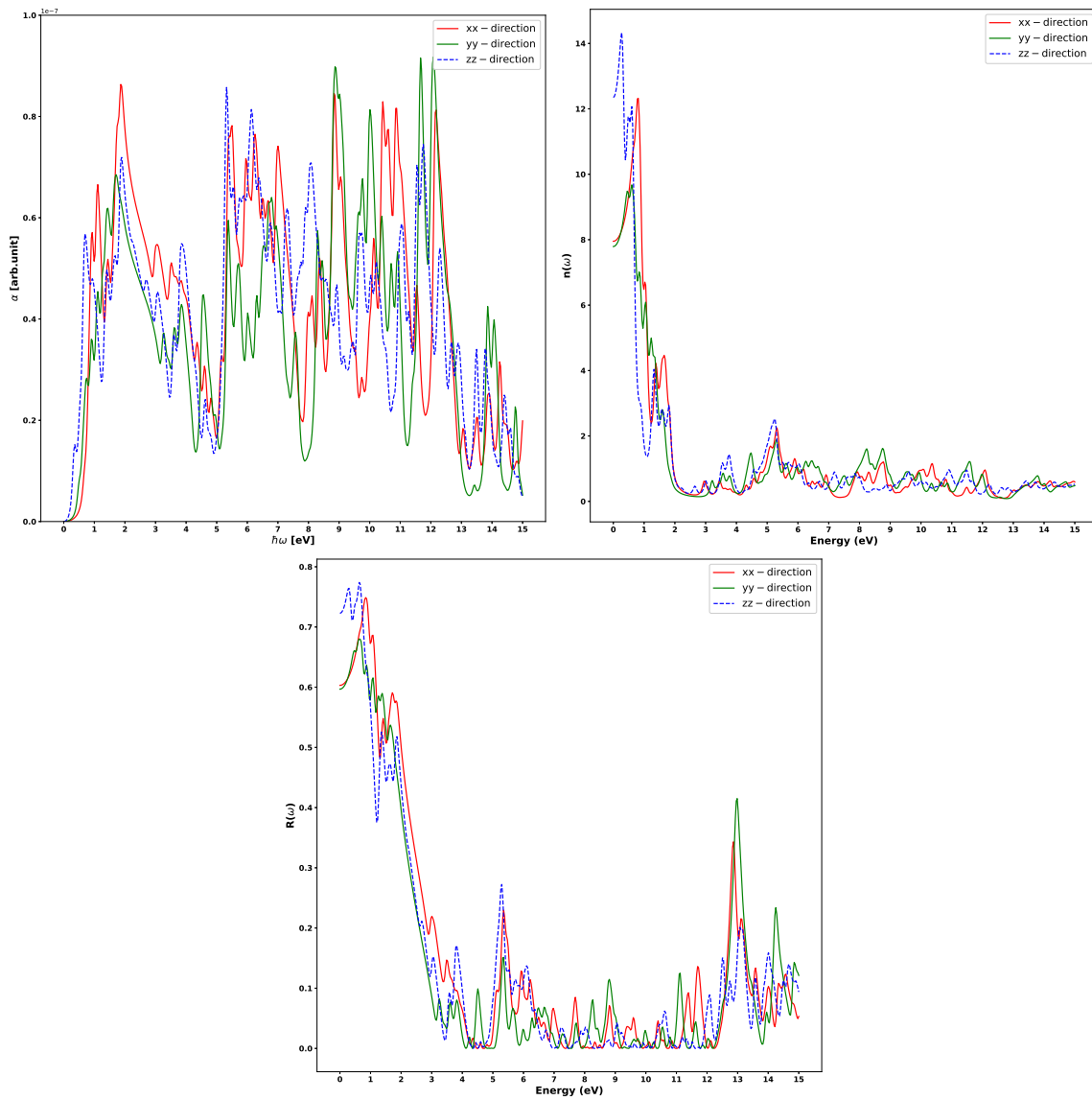


Figure 8: The graph of: (a) absorption coefficient, (b) refractive index, and (c) reflectivity, of LFP.

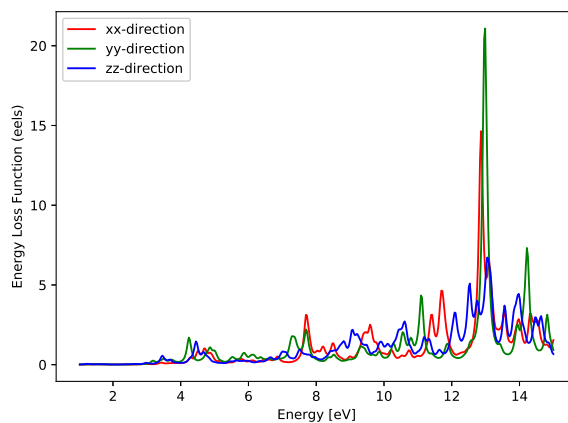


Figure 9: The electron-energy loss spectrum of LFP.

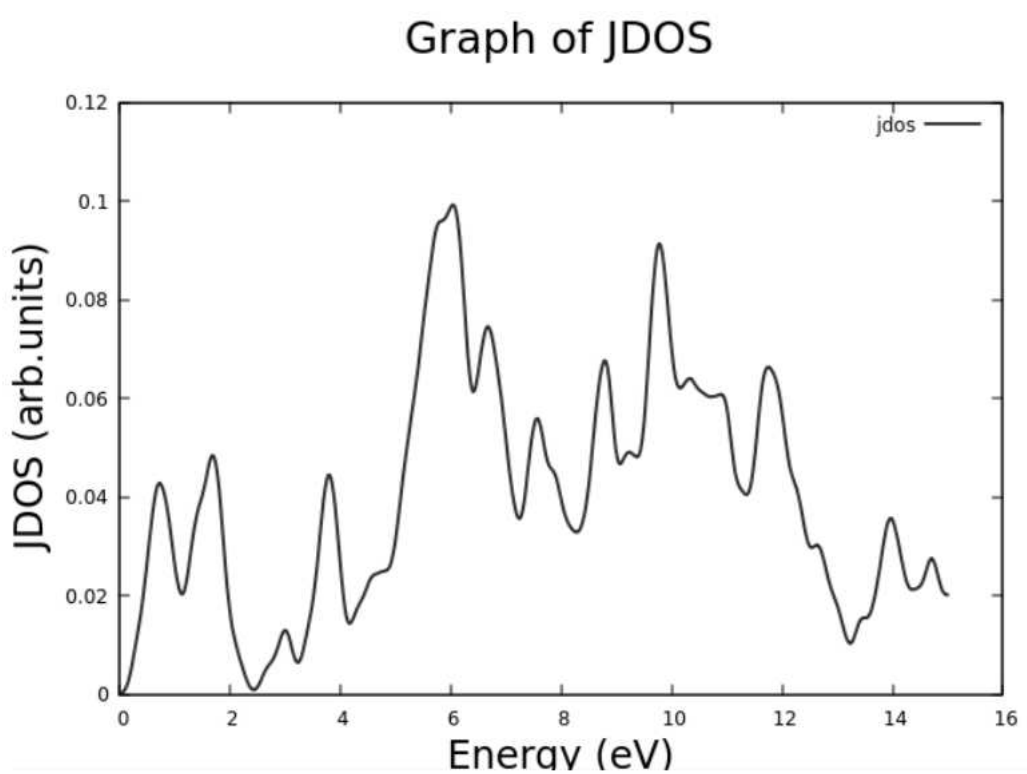


Figure 10: The joint density of states (JDOS) of LFP.

#### 4. Conclusion

In this study, we have employed a DFT + U calculations to investigate the structural, electronic, optical, and magnetic properties of LiFePO<sub>4</sub> cathode material for Li-ion batteries. We have performed the structural optimization and calculated the equilibrium parameters such as the lattice constants, and the bulk modulus using QE code and found that  $a = 4.76 \text{ \AA}$ ,  $b = 6.00 \text{ \AA}$ ,  $c = 10.28 \text{ \AA}$ , and  $\beta = 90.2 \text{ GPa}$ . The results obtained are in agreement with experimental results reported in the literature.

The result obtained with a DFT + U showed that LiFePO<sub>4</sub> is direct band gap materials with a band gap of 3.82 eV, which is within a range of the experimental values. We have analyzed the projected density of states which suggest that the majority spin states of FePO<sub>4</sub> have substantial covalent character due to the energetic overlap of the O states with the Fe states. In LiFePO<sub>4</sub>, there is less covalent character such that the Fe states form narrow bands above the O bands with a relatively lower extent of mixing. Thus, based on the results, it seems that LiFePO<sub>4</sub> is more stable than FePO<sub>4</sub>.

On the basis of the predicted optical absorbance, reflection, refractive index, and energy loss function, LiFePO<sub>4</sub> seems to be viable and cost-effective as a cathode material for Li-ion battery. Furthermore, it appears that the DFT + U formalism is the most suitable choice to investigate the strongly correlated LiFePO<sub>4</sub> system, contributing to further literature resource involving such technological material.

#### CRedit authorship contribution statement

A.K. Wabeto conducted the DFT calculations, and wrote the draft manuscript; K.N. Nigussa directed the research process and carried out the writing of the revised manuscript; and L.D. Deja supported on the research process.

#### Declaration of Competing Interest

The authors declare that they have no known competing financial interests or personal relationships that could have appeared to influence the work reported in this paper.

#### Acknowledgements

We are grateful to the Ministry of Education of Ethiopia for financial support. The authors also acknowledge the Department of Physics at Addis Ababa University. The office of VPRTT of Addis Ababa University is also warmly appreciated for supporting this research under a grant number AR/053/2021.

#### Data Availability Statement

The data that support the findings of this study are available upon reasonable request from the authors.

#### ORCID iDs

K.N. Nigussa.  
<https://orcid.org/0000-0002-0065-4325>.

## References

## References

- [1] A. Joseph, M. Shahidehpour, *Battery storage systems in electric power systems*, in: 2006 IEEE Power Engineering Society General Meeting, 2006, pp. 8–pp.  
URL <https://ieeexplore.ieee.org/document/1709235>
- [2] P. Arévalo, M. Tostado-Véliz, F. Jurado, *A novel methodology for comprehensive planning of battery storage systems*, *Journal of Energy Storage* 37 (2021) 102456.  
URL <https://doi.org/10.1016/j.est.2021.102456>
- [3] J. Figgenger, P. Stenzel, K.-P. Kairies, J. Linßen, D. Haberschusz, O. Wessels, M. Robinius, D. Stolten, D. U. Sauer, *The development of stationary battery storage systems in Germany—status 2020*, *Journal of Energy Storage* 33 (2021) 101982.  
URL <https://doi.org/10.1016/j.est.2020.101982>
- [4] A. S. Hassan, L. Cipcigan, N. Jenkins, *Optimal battery storage operation for PV systems with tariff incentives*, *Applied Energy* 203 (2017) 422–441.  
URL <https://doi.org/10.1016/j.apenergy.2017.06.043>
- [5] L. Saw, K. Somasundaram, Y. Ye, A. Tay, *Electro-thermal analysis of Lithium Iron Phosphate battery for electric vehicles*, *Journal of Power Sources* 249 (2014) 231–238.  
URL <https://doi.org/10.1016/j.jpowsour.2013.10.052>
- [6] J. Hassoun, F. Bonaccorso, M. Agostini, M. Angelucci, M. G. Betti, R. Cingolani, M. Gemmi, C. Mariani, S. Panero, V. Pellegrini, et al., *An advanced lithium-ion battery based on a graphene anode and a lithium iron phosphate cathode*, *Nano letters* 14 (8) (2014) 4901–4906.  
URL <https://doi.org/10.1021/nl502429m>
- [7] N. Omar, M. Daowd, P. Van Den Bossche, O. Hegazy, J. Smekens, T. Coosemans, J. Van Mierlo, *Rechargeable energy storage systems for plug-in hybrid electric vehicles—assessment of electrical characteristics*, *Energies* 5 (8) (2012) 2952–2988.  
URL <https://doi.org/10.3390/en5082952>
- [8] T. Satyavani, A. S. Kumar, P. S. Rao, *Methods of synthesis and performance improvement of lithium iron phosphate for high rate li-ion batteries: A review*, *Engineering Science and Technology, an International Journal* 19 (1) (2016) 178–188.  
URL <https://doi.org/10.1016/j.jestch.2015.06.002>
- [9] Y. Xiao, F. C. Zhang, J. I. Han, *Electrical structures, magnetic polaron and lithium ion dynamics in three transition metal doped  $\text{LiFe}_{1-x}\text{M}_x\text{PO}_4$  (M= Mn, Co and Ni)*, *Solid State Ionics* 294 (2016) 73–81.  
URL <https://doi.org/10.1016/j.ssi.2016.06.009>
- [10] M. H. Alfaruqi, S. Kim, S. Park, S. Lee, J. Lee, J.-Y. Hwang, Y.-K. Sun, J. Kim, *Density functional theory investigation of mixed transition metals in olivine and tavorite cathode materials for li-ion batteries*, *ACS applied materials & interfaces* 12 (14) (2020) 16376–16386.  
URL <https://doi.org/10.1021/acsami.9b23367>
- [11] S. Oukahou, A. Elomrani, M. Maymoun, K. Sbiaai, A. Hasnaoui, *Investigation of  $\text{LiMn}_{1-x}\text{M}_x\text{PO}_4$  (M= Ni, Fe) as cathode materials for Li-ion batteries using density functional theory*, *Computational Materials Science* 202 (2022) 111006.  
URL <https://doi.org/10.1016/j.commatsci.2021.111006>
- [12] Q. He, B. Yu, Z. Li, Y. Zhao, *Density functional theory for battery materials*, *Energy & Environmental Materials* 2 (4) (2019) 264–279.  
URL <https://doi.org/10.1002/eem2.12056>
- [13] M. Nakayama, S. Yamada, R. Jalem, T. Kasuga, *Density functional studies of olivine-type  $\text{LiFePO}_4$  and  $\text{NaFePO}_4$  as positive electrode materials for rechargeable lithium-ion batteries*, *Solid State Ionics* 286 (2016) 40–44.  
URL <https://doi.org/10.1016/j.ssi.2015.12.019>
- [14] J. E. Saal, S. Kirklin, M. Aykol, B. Meredig, C. Wolverton, *Materials design and discovery with high-throughput density functional theory: the open quantum materials database*, *Computational Materials Science* 65 (2013) 1501–1509.  
URL <https://doi.org/10.1007/s11837-013-0755-4>
- [15] P. Giannozzi, S. Baroni, N. Bonini, M. Calandra, R. Car, C. Cavazzoni, D. Ceresoli, G. L. Chiarotti, M. Cococcioni, I. Dabo, A. D. Corso, S. de Gironcoli, S. Fabris, G. Fratesi, R. Gebauer, U. Gerstmann, C. Gougoussis, A. Kokalj, M. Lazzeri, L. Martin-Samos, N. Marzari, F. Mauri, R. Mazzarello, S. Paolini, A. Pasquarello, L. Paulatto, C. Sbraccia, S. Scandolo, G. Sclauzero, A. P. Seitsonen, A. Smogunov, P. Umari, R. M. Wentzcovitch, *QUANTUM ESPRESSO: a modular and open-source software project for quantum simulations of materials*, *Journal of Physics: Condensed Matter* 21 (2009) 395502.  
URL <https://doi.org/10.1088/0953-8984/21/39/395502>
- [16] P. Blöchl, *Projector augmented-wave method*, *Phys. Rev. B* 50 (1994) 17953.  
URL <https://doi.org/10.1103/PhysRevB.50.17953>
- [17] L. Kleinman, D. M. Bylander, *Efficacious form for model pseudopotentials*, *Phys. Rev. Lett.* 48 (1982) 1425–1428.  
URL <https://link.aps.org/doi/10.1103/PhysRevLett.48.1425>
- [18] J. Perdew, K. Burke, M. Ernzerhof, *Generalized Gradient Approximation Made Simple*.
- [19] H. Monkhorst, J. Pack, *Special points for Brillouin-zone integrations*, *Phys. Rev. B* 13 (1976) 5188.  
URL <https://doi.org/10.1103/PhysRevB.13.5188>
- [20] H. Schlegel, *Optimization of equilibrium geometries and transition structures*, *J. Comp. Chem.* 3 (1982) 214.  
URL <https://doi.org/10.1002/jcc.540030212>
- [21] P. Feynman, *Forces in Molecules*, *Phys. Rev.* 56 (1939) 340.  
URL <https://doi.org/10.1103/PhysRev.56.340>

- [22] O. Nielsen, R. Martin, [Quantum-mechanical theory of stress and force](https://doi.org/10.1103/PhysRevB.32.3780), Phys. Rev. B. 32 (1985) 3780.  
URL <https://doi.org/10.1103/PhysRevB.32.3780>
- [23] R. Wentzcovitch, J. Martins, [First principles molecular dynamics of Li: Test of a new algorithm](https://doi.org/10.1016/0038-1098(91)90629-A), Solid State Commun. 78 (1991) 831.  
URL [https://doi.org/10.1016/0038-1098\(91\)90629-A](https://doi.org/10.1016/0038-1098(91)90629-A)
- [24] S. Grimme, S. Ehrlich, L. Goerigk, [Effect of the damping function in dispersion corrected density functional theory](https://doi.org/10.1002/jcc.21759), Journal of Computational Chemistry 32 (2011) 1456.  
URL <https://doi.org/10.1002/jcc.21759>
- [25] V. I. Anisimov, J. Zaanen, O. K. Andersen, [Band theory and Mott insulators: Hubbard U instead of Stoner I](https://link.aps.org/doi/10.1103/PhysRevB.44.943), Phys. Rev. B 44 (1991) 943–954.  
URL <https://link.aps.org/doi/10.1103/PhysRevB.44.943>
- [26] M. Hybertsen, S. Louie, [Ab initio static dielectric matrices from the density-functional approach: Formulation and application to semiconductors and insulators](https://doi.org/10.1103/PhysRevB.35.5585), Phys. Rev. B 35 (1987) 5585.  
URL <https://doi.org/10.1103/PhysRevB.35.5585>
- [27] M. Gajdoš, K. Hummer, G. Kresse, J. Furthmüller, F. Bechstedt, [Linear optical properties in the projector-augmented wave methodology](https://doi.org/10.1103/PhysRevB.73.045112), Phys. Rev. B 73 (2006) 045112.  
URL <https://doi.org/10.1103/PhysRevB.73.045112>
- [28] F. Wooten, *Optical Properties of Solids*, Academic Press, New York, 1972.
- [29] S. Saha, T. P. Sinha, A. Mookerjee, [Electronic structure, chemical bonding, and optical properties of paraelectric BaTiO<sub>3</sub>](https://link.aps.org/doi/10.1103/PhysRevB.62.8828), Phys. Rev. B 62 (2000) 8828.  
URL <https://link.aps.org/doi/10.1103/PhysRevB.62.8828>
- [30] R. Norris, K. Iyer, V. Chabot, P. Nieva, A. Yu, A. Khajepour, J. Wang, [Multi-band reflectance spectroscopy of carbonaceous lithium iron phosphate battery electrodes versus state of charge](https://doi.org/10.1117/12.2222222), in: *Optical Components and Materials XI*, Vol. 8982, SPIE, 2014, pp. 260–267.
- [31] R. Li, S. Wu, Y. Yang, Z. Zhu, [Structural and electronic properties of Li-ion battery cathode material FeF<sub>3</sub>](https://doi.org/10.1016/j.jssc.2015.03.019), The Journal of Physical Chemistry C 114 (39) (2010) 16813–16817.  
URL <https://doi.org/10.1016/j.jssc.2015.03.019>
- [32] H. Yousefi-Mashhour, A. Namirani, M. M. Kalantarian, [A first principle study of structural and electrical properties of novel Li<sub>2</sub>FeO<sub>3</sub>/Li<sub>2</sub>FeO<sub>2</sub>F Li-ion battery](https://doi.org/10.3390/en12020224), Low Temperature Physics 49 (1) (2023) 38–45.  
URL <https://doi.org/10.3390/en12020224>
- [33] F. Murnaghan, [The Compressibility of Media under Extreme Pressures](https://doi.org/10.1073/pnas.30.9.244), Proc. Natl. Acad. Sci. 30 (1944) 244.  
URL <https://doi.org/10.1073/pnas.30.9.244>
- [34] F. C. Strobridge, D. S. Middlemiss, A. J. Pell, M. Leskes, R. J. Clément, F. Pourpoint, Z. Lu, J. V. Hanna, G. Pintacuda, L. Emsley, et al., [Characterising local environments in high energy density Li-ion battery cathodes: a combined NMR and first principles study of LiFe<sub>x</sub>Co<sub>1-x</sub>PO<sub>4</sub>](https://doi.org/10.1039/C4TA00934G), Journal of Materials Chemistry A 2 (30) (2014) 11948–11957.  
URL <https://doi.org/10.1039/C4TA00934G>
- [35] Z. Yang, Y. Pei, X. Wang, L. Liu, X. Su, [First principles study on the structural, magnetic and electronic properties of Co-doped FeF<sub>3</sub>](https://doi.org/10.1063/1.5085162), Computational and Theoretical Chemistry 980 (2012) 44–48.  
URL <https://doi.org/10.1063/1.5085162>
- [36] R. Bader, *Atoms in Molecules: A Quantum Theory*, Oxford University Press, New York, 1990.  
URL <https://doi.org/10.1126/science.252.5012.1566.b>
- [37] W. Tang, E. Sanville, G. Henkelman, [A grid-based Bader analysis algorithm without lattice bias](https://doi.org/10.1088/0953-8984/21/8/084204), J. Phys.: Condens. Matter 21 (2009) 084204.  
URL <https://doi.org/10.1088/0953-8984/21/8/084204>
- [38] J. Kuriplach, A. Pulkkinen, B. Barbiellini, [First-principles study of the impact of grain boundary formation in the cathode material LiFePO<sub>4</sub>](https://doi.org/10.1088/1361-6480/ab1111), Condensed Matter 4 (3) (2019) 80.
- [39] L. J. Miara, W. D. Richards, Y. E. Wang, G. Ceder, [First-principles studies on cation dopants and electrolyte— cathode interphases for lithium garnets](https://doi.org/10.1021/acs.chemmater.5b01023), Chemistry of Materials 27 (11) (2015) 4040–4047.  
URL <https://doi.org/10.1021/acs.chemmater.5b01023>
- [40] G. Ceder, G. Hautier, A. Jain, S. P. Ong, [Recharging lithium battery research with first-principles methods](https://doi.org/10.1557/mrs.2011.31), Mrs Bulletin 36 (2011) 185–191.  
URL <https://doi.org/10.1557/mrs.2011.31>
- [41] M.-F. Ng, M. B. Sullivan, [First-principles characterization of lithium cobalt pyrophosphate as a cathode material for solid-state Li-ion batteries](https://doi.org/10.1021/acs.jpcc.9b09946), The Journal of Physical Chemistry C 123 (49) (2019) 29623–29629.  
URL <https://doi.org/10.1021/acs.jpcc.9b09946>
- [42] S. P. Ong, *First principles design and investigation of Lithium-Ion battery cathodes and electrolytes*, Department of Materials Science and Engineering.